APPLICATION **NOTE**

cadence®

Design of a BAW Quadplexer Module Using AWR Software

With the development of the LTE-Advanced and orthogonal frequency division multiple access (OFDMA) techniques, multiple carrier technology has become important in the mobile communication industry. Designers are meeting the challenge of working with multi-carrier signal-frequency systems by using diplexers and duplexers in RF circuits to separate different carriers. For example, two carrier signals can be separated by using a diplexer. The transmit (TX) and receive (RX) aggregated-carrier functionality is greatly enhanced by compact-designed duplexers and multiplexers.

This application note describes the design of a carrier aggregation (CA) bulk acoustic wave (BAW) quadplexer module. The module is intended for the LTE-3 and LTE-7 bands, with high in-band and cross-band isolation. Qorvo TQQ1003 and TQQ1007 BAW duplexers were used for the duplexer and the circuit was designed with the Cadence® AWR Design Environment® platform, specifically Cadence AWR® Microwave Office® circuit design software. The design is described in steps: filter, T-junction, diplexer, and quadplexer.

CA Technology

Figure 1 shows the general working structure of CA technique.

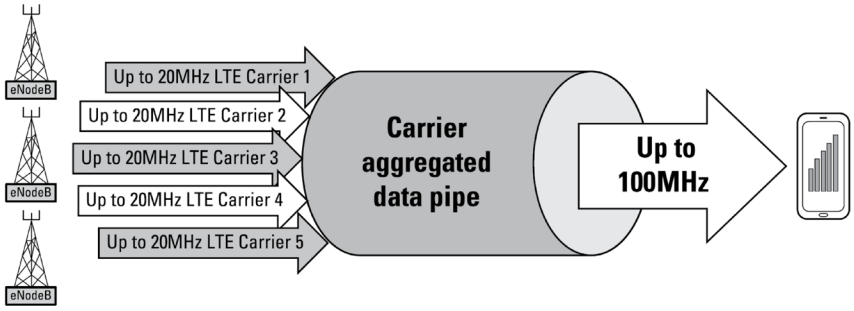

Figure 1: Working mechanism of the CA (image courtesy of Qorvo)

CA technology can incorporate carriers of different (inter-band) frequency bands, as well as carriers of the same (intra-band) frequency bands, and carriers in the same frequency band can be either intra-band contiguous or non-contiguous. The easiest way to arrange aggregation would be to use contiguous component carriers within the same operating frequency band (as defined for LTE), called intraband contiguous. This might not always be possible, due to operator frequency allocation scenarios, in which case non-contiguous carriers can be employed. In fact, non-contiguous frequency allocation is the more commonly-used technique, which is advantageous since filter technology used for separating carriers often performs better for non-contiguous signals than for contiguous signals. In addition, it is far more difficult to use inter-band (different band) carriers since processing these signals requires complicated and advanced TX and RX structures. Figure 2 shows frequency allocation of the intraband and interband carriers.[1]

Figure 2: Allocation of the intra-band contiguous (left) and inter-band carriers (right) (image courtesy of Qorvo)

BAW Filter Technology

BAW technology enables designers to create narrowband filters with exceptionally steep filter skirts and excellent rejection. This makes BAW the technology of choice for many challenging interference problems. BAW delivers these benefits at frequencies above 1.5GHz up to 6GHz and is used for many of the new LTE bands above 1.9GHz, making it a complementary technology to surface acoustic wave (SAW), which is most effective at lower frequencies, but scaled down in size. A piezo-electric film is sandwiched between two metal films as shown in Figure 3. The equivalent Butterworth/VanDyke circuit model consists of a fixed structure capacitance in parallel with a frequency dependent electro-mechanical resonant circuit. In the Van Dyke model[2] shown in Figure 3 (left), the series and parallel cascaded BAW resonators are arranged in a ladder configuration. The passband frequency is tuned by modifying the shunt resonators.

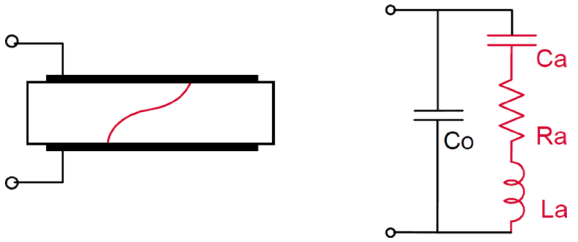

Figure 3: BAW resonator (left) and BAW cross-section (right) of a Van Dyke model

In the design presented in this application note, the BAW filters were configured into a quadplexer design, which was simulated and realized to work with B3 and B7 LTE bands, covering between 1710MHz and 1880MHz and between 2500MHz and 2690MHz, respectively. Two BAW duplexers were used in order to separate the TX and RX signals at the bands. Specifications for the quadplexer were high in-band and cross-band isolation, good reflection loss (below 10dB), and fine insertion low above -6dB. Figure 4 shows the basic circuit structure and ports defining the quadplexer.

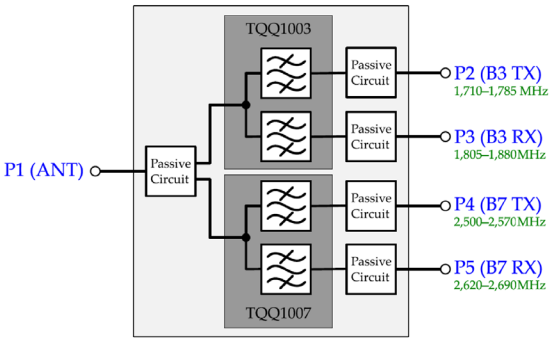

Figure 4: Schematic of the quadplexer module

General Structure of the Quadplexer

The quadplexer is developed by combining two duplexers via a diplexer that consists of two filters. In order to design the quadplexer, the S-parameters of the BAW duplexers provided in a Touchstone file were processed using AWR Microwave Office software. Two options were evaluated for the creation of the common node for the two duplexers. One option was to design a power divider/combiner based on a coupler that splits and combines input power to and from the duplexers. An ideal coupler would introduce an additional 3dB of insertion loss for all frequencies, which was not desirable because of the two-fold increase in the overall insertion loss. Option two was to design a frequency divider that switches lower frequencies to one path and higher frequencies to another path, thereby avoiding much of the 3dB power loss incurred with a passive coupler architecture. Once the system requirements of the quadplexer were defined, the diplexer and other network details were designed. From the common node to the duplexers, the diplexer consisted of several sections, such as filters, matching networks, and T-junctions. Figure 5 shows the general circuit model.

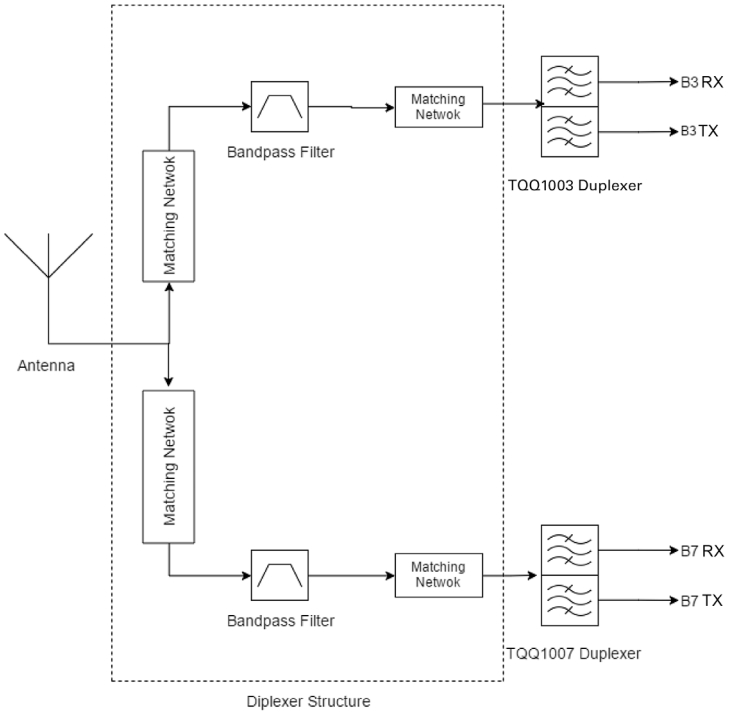

Figure 5: General structure of the quadplexer

Filter

Diplexers are often required for dual-band operation; therefore, the diplexer is a key component in the transceiver module. Since diplexers are intended for use in handheld devices and personal communication systems, they need to be as compact and planar as possible, and the common procedure is to combine two bandpass filters (BPFs) via an optimized T-junction.[3] It is important to design the BPFs for low insertion loss, the appropriate bandwidth, selectivity, and out-of-band rejection. In addition, the isolation of the overall system is an important parameter in order to avoid unnecessary loading at the front-end devices. BPFs present controllable transmission zeros, which is the frequency at which the transfer function of a linear two-port network has zero transmission. This ensures an acceptable stopband rejection is available to maximize isolation between crossbands (TX/RX frequencies).

Figure 6 shows the structure of the proposed diplexer, which consists of two BPFs, a stepped-impedance resonator (SIR), and a matching circuit between filters combined at the antenna port with a T-junction/matching structure. The T-junction is typically used in a combining circuit and requires careful design of the width and length of the microstrip transmission lines, which was accomplished using AWR Microwave Office software.[4]

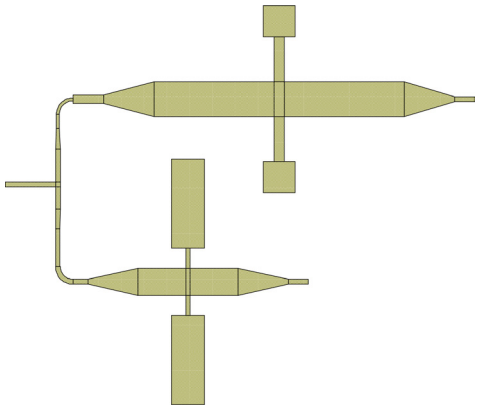

Figure 6: Structure of the proposed diplexer

The center frequencies of designed BPFs were 1.8GHz and 2.6GHz for the B3 and B7 LTE bands, respectively. There was a tradeoff between the order and dimensions of the filters. In order to constrain the size, a first-order Chebyshev filter was preferred due to the fewer number of reactive components, low ripple at the passband, and steep roll-off at the skirt of the transition bands.[4] In order to design the BPF, one transmission line and two stepped-impedance open stubs were used because they generated two transmission zeros near the passband frequency[5] and the bandwidth of the filters could be easily controlled by relocating those transmission zeros. The two stepped-impedance stubs provided low loss, good selectivity, and a steep transition band. Figure 7 shows the configuration of the stepped-impedance model, where each step equals a λ/4 electrical length at the center frequency of the filter and Z1 and Z2 are the impedance of each segment.

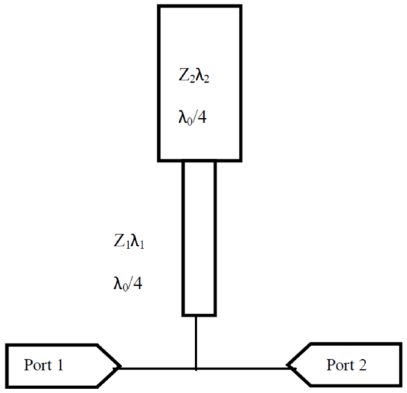

Figure 7: Stepped-impedance open stub

The line width and length of the microstrip transmission lines were calculated according to the electrical length of the quarter-wave length for a Rogers Duroid 6010 substrate with a dielectric constant of 10.8 and thickness of 0.635mm. The calculations were made using the TX-LINE transmission-line calculator in AWR Microwave Office software. Two identical stepped-impedance open stubs were used in order to increase the stopband rejection ratio. Figure 8 shows the filter parameters of BPF for the B3 band with center frequency of 1.8GHz in AWR Microwave Office software.

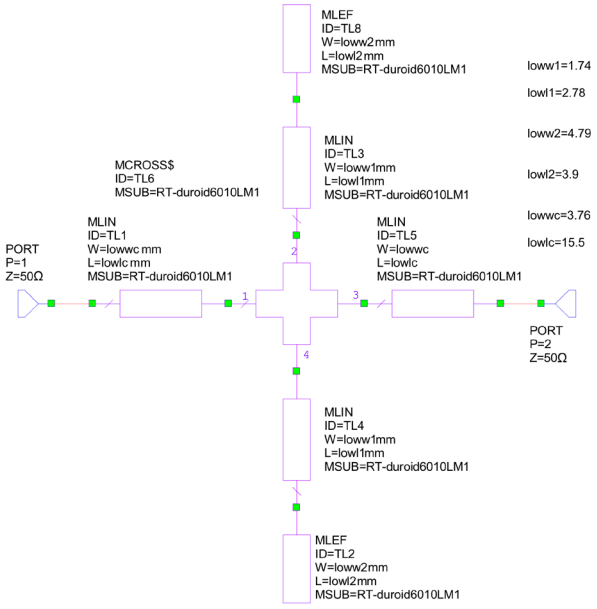

Figure 8: Filter parameters of the BPF for the B3 LTE band

After the element variables were calculated and estimated, the next step was simulation. Two simulation approaches were considered. One is a linear simulation in which overall system parameters are calculated by separately cascading the S-parameters of each of the elements. This simulation provides insight about the circuit performance and matching characteristics of the elements. The second approach is to use electromagnetic (EM) simulation to analyze overall circuit behavior, validating the accuracy of the individual transmission line elements and their use in this modeling effort, and addressing any non-modeled parasitics such as coupling effects.

Both approaches account for substrate features such as height of the substrate, height of the open space above the layout, and non-idealities of the conductor. After initially developing the circuit parameters (line widths, lengths) using the schematic-based transmission line elements, it was decided that the EM simulation approach would provide better accuracy and insight about circuit behavior after manufacturing.

Figure 9 shows the S-parameters of the B3 LTE BPF The S11 parameters show the reflection loss as well as the matching characteristics. The S21 parameters show the insertion loss over frequency in which some signals are attenuated more than others due to the intended filtering.

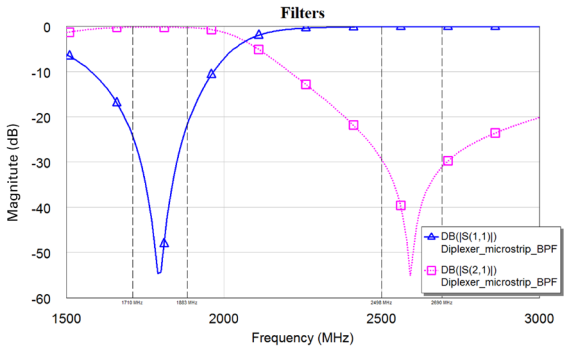

Figure 9: S-parameter results of the EM simulation for the B3 LTE BPF

As shown in the Figure 9, the BPF for the B3 band at 1.8GHz has excellent return loss (below 20dB) and transmission zero (band rejection) at the B7 band (2.6GHz), which will provide satisfactory isolation for the diplexer. Circuit elements and variables of the B7 LTE band BPF are shown in Figure 10. The two filters have similar circuit layout with different dimensions.

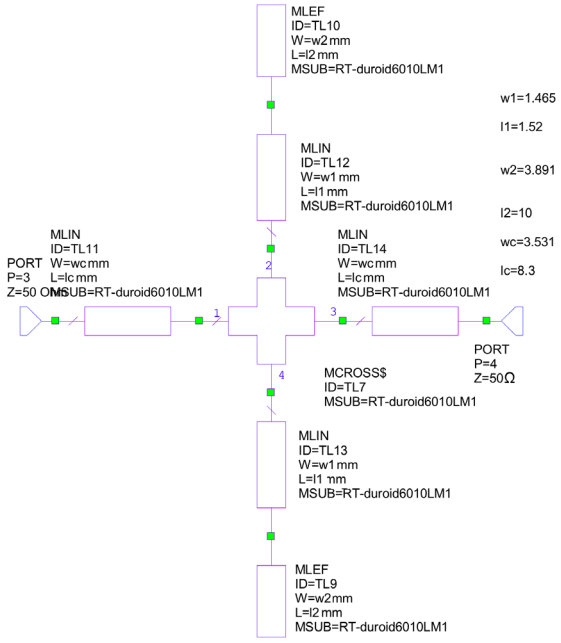

Figure 10: Circuit elements and variables of the B7 band BPF

The simulation results for the B7 band BPF are shown in Figure 11. Transition zero is adjusted to be in the counter-frequency band in order to have favorable isolation in the diplexer.

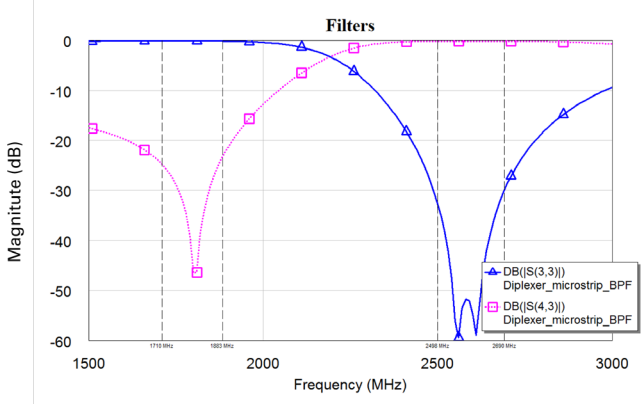

Figure 11: S-parameters of the EM simulation results for the B7 BPF

Looking at the insertion losses of the both filters, it can be seen that the signal has very little attenuation over the bands and that the reflection of the filter has been kept to a minimum. The next step was to combine the two BPFs with a T-junction in order to create a diplexer.

T-Junction

The matching network and combining filters ensured that both filters are matched to the common node and had acceptable isolation between them. The two circuits were combined using a T-junction with a feasible tuning impedance via length and width of transmission lines. The T-shaped connector had two transmission line sections at both ends. It was decided to provide a high, preferably infinite, impedance for Filter A at the load of Filter B for that particular frequency, and vice versa. Figure 12 shows the circuit model of the T-junction.

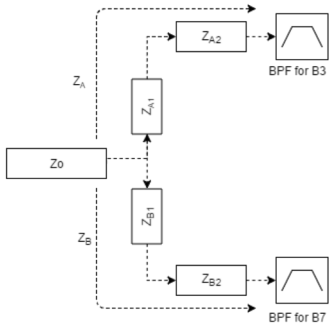

Figure 12: The T-junction model circuit with impedance notations

The input impedance of the T-junction was required to meet the following criteria in order to achieve satisfactory impedance matching:

$$Z_A = \begin{cases} \infty \text{ (open) at } 2.6\text{GHz} \\ 50\ \Omega \text{ at } 1.8\text{GHz} \end{cases}$$
$$Z_B = \begin{cases} \infty \text{ (open) at } 1.8\text{GHz} \\ 50\ \Omega \text{ at } 2.6\text{GHz} \end{cases}$$

Z_A and Z_B are the input impedance of the input of diplexer at the junction looking into the lower and the upper part.[3] Z_{A1} and Z_{B1} are the 50Ω microstrip transmission lines that transform the low impedance at the input to the open circuit for counter frequency for both sides. Z_{A2} and Z_{B2} are the high impedance microstrip transmission lines which are combined with the 50Ω lines in order to increase the effective impedance of the input.[4] Figure 13 shows the circuit element dimensions that satisfy the equation criteria.

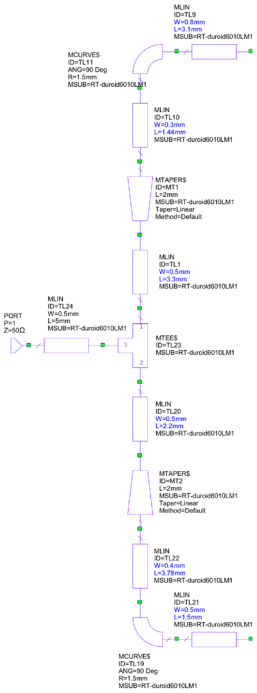

Figure 13: Circuit elements and dimensions of the T-junction

Figure 14 shows the real and imaginary impedance values of the T-junction. The equation is satisfied in order to connect the two filters into the common node.

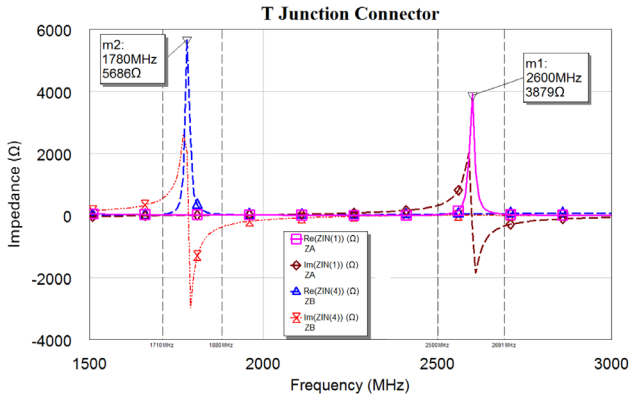

Figure 14: Real and imaginary impedance of the T-junction inputs

Diplexer

After designing the two BPFs and the T-junction, the next step was to connect the two BPFs to the T-function and run the EM simulation. Figure 15 shows the circuit elements and variables. It can be seen that connecting the two filters to the common node is an easy process using the T-junction.

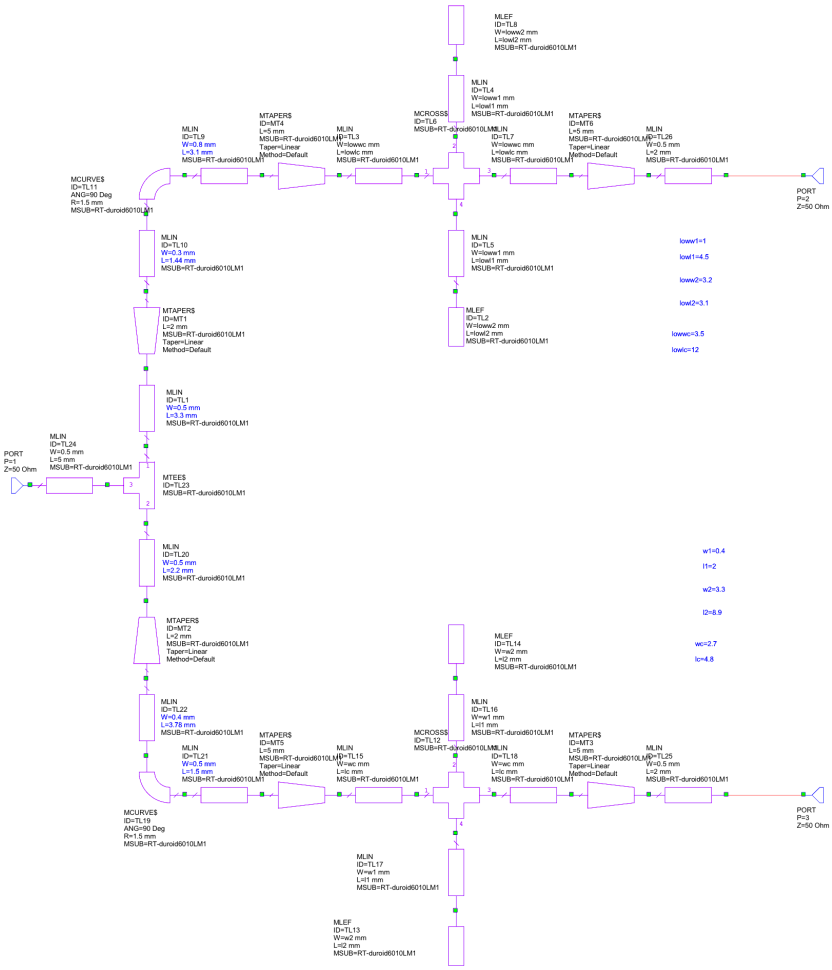

Figure 15: Circuit elements and variables of the diplexer

The approximate width of the T-junction is 0.4mm and the width of the BPFs is about 4mm. To prevent width mismatch between two transmission lines, tapered transmission lines were used. After adding these tapered lines, some lengths needed fine tuning since the length of the tapered line affects circuit behavior. Figure 16 shows the S11 and S23 parameters, which indicate reflection loss and isolation loss, respectively.

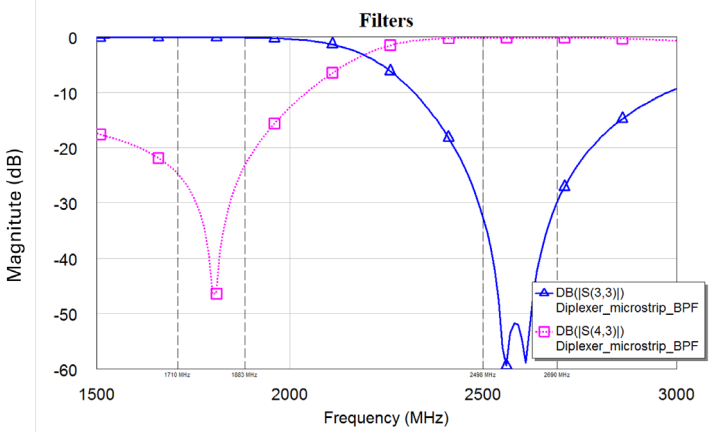

Figure 16: Reflection loss and isolation loss of the diplexer

It can be seen that the isolation of the bands has its lowest point at the transmission zero of the BPFs These properties provided acceptable isolation for the diplexer. EM simulation results shows reflection loss of the signal at the B3 and B7 frequency bands is around -20dB. These values were considered realistic in order to have acceptable reflection loss after manufacturing.

Figure 17 shows the insertion loss parameters of Ports 2 and 3, shown as the S21 and S31 parameters. Out-band rejection of the diplexer is above acceptable. The lowest insertion loss for the in-band is around -0.4dB, which is an acceptable level of insertion loss at that band. The simulation of the diplexer showed acceptable design parameters. The next step was to combine the two duplexers to create the quadplexer.

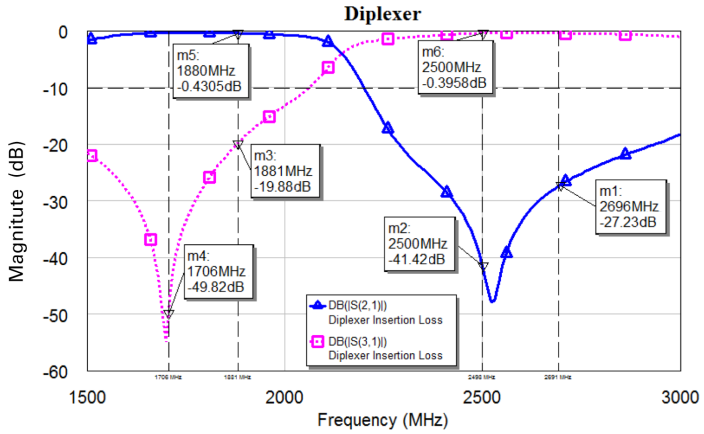

Figure 17: Insertion loss of the diplexer

Quadplexer

Before combining the BAW duplexer to a common node via the diplexer, it was necessary to evaluate the S-parameters of the BAW duplexers. Figure 18 (left) shows the S-parameters of the duplexer for the B3 LTE band. The S-parameters of the module are the same as the datasheet.[6] Figure 18 (right) shows the S-parameters of the B7 LTE band duplexer. The S-parameters of the module are the same as the datasheet.[7]

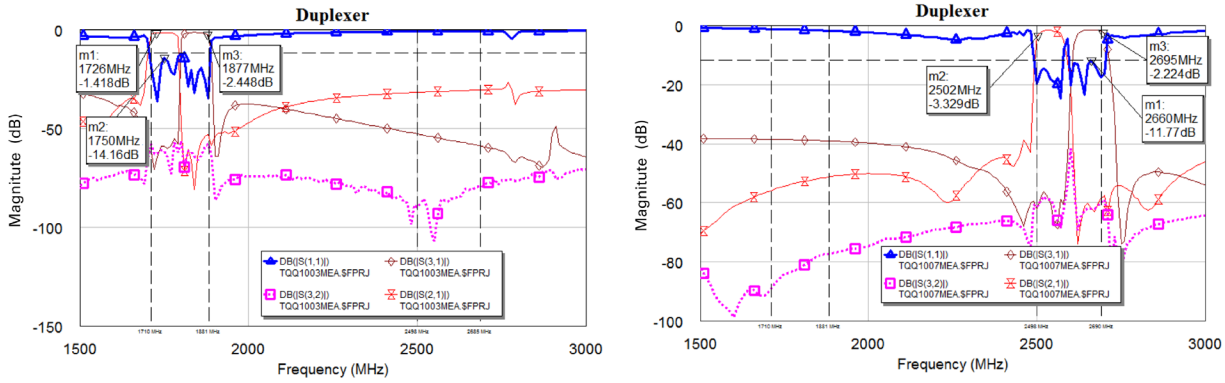

Figure 18: S11 and S32 parameters of the BAW duplexer (left) and S-parameters of the band 7 BAW duplexer (right)

Because the BAW filters were matched to 50Ω, the diplexer and duplexer were easily connected as a cascade structure. The small packet dimensions and pad width needed additional attention to the connection of the BPF`s 4mm-wide transmission line to the BAW duplexer`s 0.35mm-wide pad. In order to eliminate mismatch of these transmission lines, tapered microstrip transmission lines were used.

Because the circuit was designed to be small and compact, the SubMiniature version A (SMA) connectors of the circuit were placed as close together as possible. The circuit had dimensions of 5x4cm length and width. After the circuit elements were placed in the layout, an EM simulation was performed. Figure 19 (left) shows the simulation results for reflection loss parameters S11, S22, S33, S44, and S55 scattering parameters. It can be seen that the reflection parameters of system are around -10dB, which is an acceptable range for reflection loss. Figure 19 (right) shows the simulation results of quadplexer for insertion loss. It can be seen that the insertion loss of the diplexer has minimal effect on insertion loss of the overall system.

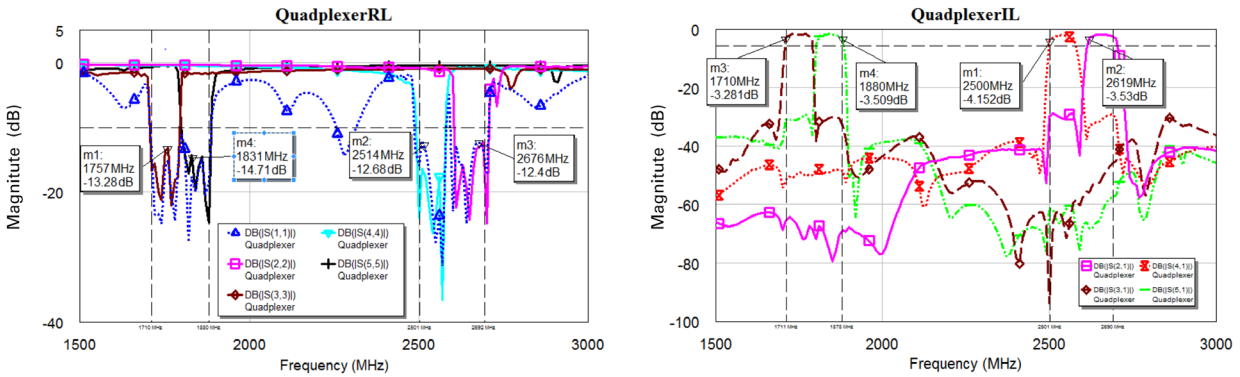

Figure 19: Simulation results of the quadplexer for reflection loss (left) and insertion loss (right)

Figure 20 shows the simulation results for the isolation of the system. The isolation was intended to be kept around -30dB; therefore, the RX or TX signal does not over drive the front-end devices. S32 and S54 indicate the in-band isolation, while S53, S52, S42, and S43 indicate the cross-band isolation.

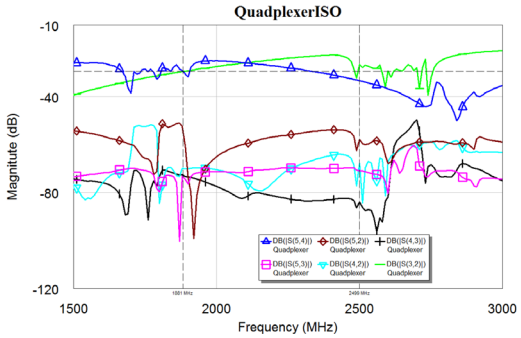

Figure 20: Simulation results of the EM simulation for in-band and cross-band isolation

The simulation results were satisfactory and proved that the quadplexer had been designed correctly. After the layout of the circuit was prepared, the next step was to design the layout of the circuit for manufacturing. In order to eliminate crosstalk of the adjacent channels, the transmission lines to the ports were separated as much as possible. It was also important to consider that the stepped impedance resonator could affect the resonance frequency. To prevent unintended resonance, the resonators were carefully placed.

Measurement Results

Measurements were performed with a Rohde & Schwarz FSH8 vector network analyzer. Figure 21 shows the measurement results for insertion loss. It can be seen that there is discontinuity at the B7 TX band, where the lowest performance was achieved at around 2.66GHz.

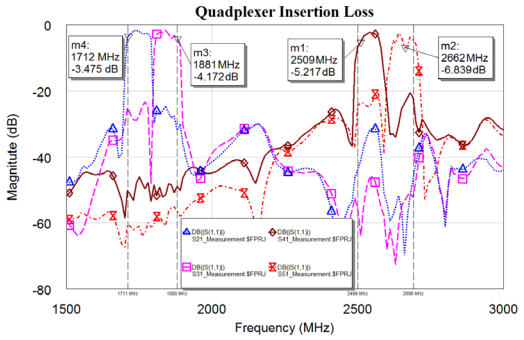

Figure 21: Simulation results for insertion loss of the quadplexer

The final measurement was the isolation loss of the quadplexer. which is shown in Figure 22. Cross-band isolation is at a satisfactory level, but in-band isolation is worse than the EM simulation result. In-band isolation is around -20dB, where expected isolation is around -30dB.

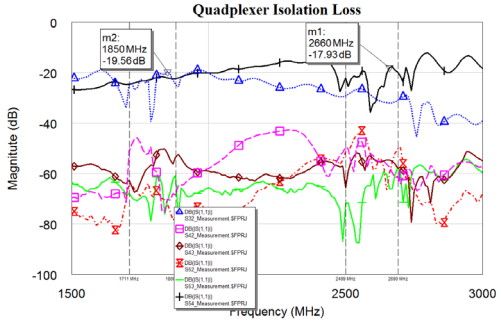

Figure 22: Measurement results for isolation of the quadplexer

Conclusion

This application example has described the design of a quadplexer with high isolation losses between output ports as realized by circuit simulation and optimization with AWR Microwave Office® software. The device slightly under performed compared to simulation results. However, there are several contributing factors, including that the quality of the machinery system was low for producing high-quality RF circuits and that the soldering process in manufacturing is challenging. While the reflection parameters are not good enough for both business and academic applications, if the diplexer is well designed, the insertion loss of the quadplexer should not be affected compared to insertion losses of the BAW duplexers, individually.

Because CA technology is used generally in mobile devices, a quadplexer or multiplexer design must be as small as possible. Another improvement point for a better quadplexer would be to use a high Q resonator rather than a stepped-impedance resonator, which would be useful in terms of selectivity and shrinking dimensions.

References

1. L. Miller, "Understanding Carrier Aggregation (CA) Technology," *Carrier Aggregation Fundamentals*, New Jersey, John Wiley & Sons, Inc., 2016, pp. 6 - 12.
2. S. Mahon ve R. Aigner, "Bulk Acoustic Wave Devices – Why, How, and Where They are Going," CS MANTECH Conference, 2007.
3. T. Yang, P.-I. Chi ve T. Itoh, "High Isolation and Compact Diplexer," *IEEE MICROWAVE AND WIRELESS COMPONENTS LETTERS*, cilt 20, no. 10, pp. 551-555, 2010.
4. R. Brinda ve P. Parveen, "Design of RF Diplexer for Mobile Communication," *International Journal of Computer Applications*, cilt 85, no. 4, pp. 16-21, 2014.
5. C. Quendo, E. Rius ve C. Person, "Narrow Bandpass Filter Using Dual-Behavior Resonators," *IEEE Trans. Microw. Theory Tech.*, cilt 51, no. 3, pp. 734-743, 2003.
6. TriQuint Semiconductor Inc, "TQQ1003 Band 3 BAW Duplexer," Qorvo Inc, 2015.
7. TriQuint Semiconductor Inc, "TQQ1007 Band 7 BAW Duplexer," Qorvo Inc, 2015.

Acknowledgment

Special thanks to Emrecan Gidik, Istanbul Technical University, for his BSc thesis, "Carrier Aggregation BAW Quadplexer Module," which inspired the creation of this application note.

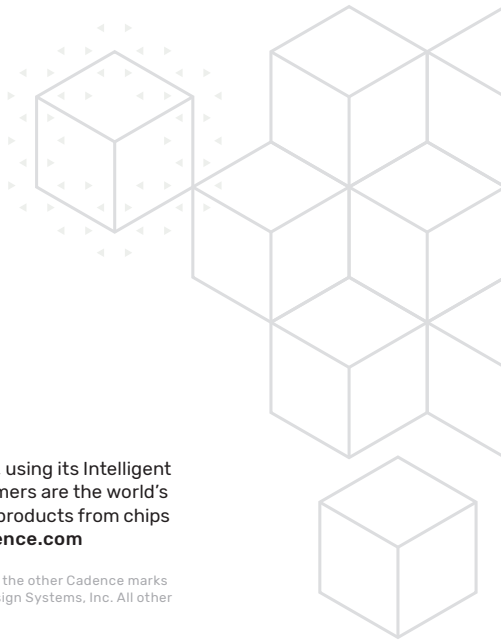

cadence®

Cadence is a pivotal leader in electronic design and computational expertise, using its Intelligent System Design strategy to turn design concepts into reality. Cadence customers are the world's most creative and innovative companies, delivering extraordinary electronic products from chips to boards to systems for the most dynamic market applications. **www.cadence.com**